AD-A063 463 ARMY ARMAMENT RESEARCH AND DEVELOPMENT COMMAND ABERD--ETC F/G 20/7
ANALYSIS OF COUPLING REGION IN TRANSMISSION-LINE ACCELERATORS.(U)
NOV 78 J K TEMPERLEY

UNCLASSIFIED ARBRL-TR-02120 SBIE-AD-E430 156 NL

1 OF 1
AD
A063463

END
DATE
FILMED
3-79
DDC

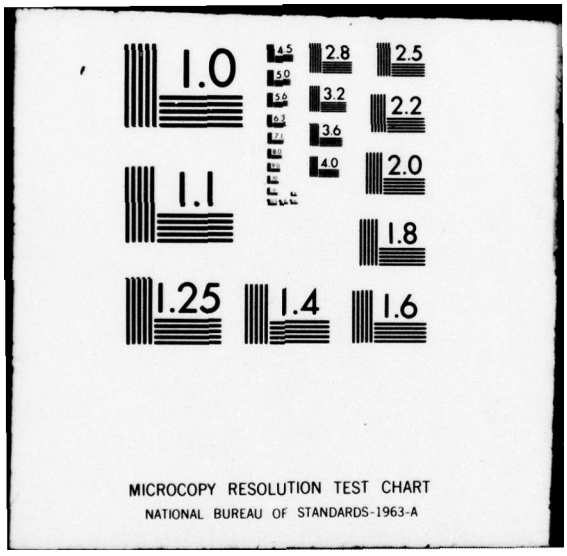
1.0
1.1
1.25
1.4
1.6
1.8
2.0
2.2
2.5
2.8
3.2
3.6
4.0
4.5
5.0
5.6
6.3
MICROCOPY RESOLUTION TEST CHART
NATIONAL BUREAU OF STANDARDS-1963-A

(12) LEVEL II

AD-E300 [illegible]

[illegible]

ANALYSIS OF [illegible]
TRANSMISSION [illegible]

(18) SBIE (19) AD-E430 156

UNCLASSIFIED

SECURITY CLASSIFICATION OF THIS PAGE (When Data Entered)

REPORT DOCUMENTATION PAGE	READ INSTRUCTIONS BEFORE COMPLETING FORM
1. REPORT NUMBER: TECHNICAL REPORT ARBRL-TR-02120 (14)	2. GOVT ACCESSION NO.
3. RECIPIENT'S CATALOG NUMBER (9)	
4. TITLE (and Subtitle) (6): ANALYSIS OF COUPLING REGION IN TRANSMISSION-LINE ACCELERATORS	5. TYPE OF REPORT & PERIOD COVERED: Final Report, Oct 77 — Jun 78
6. PERFORMING ORG. REPORT NUMBER	
7. AUTHOR(s) (10): J.K. Temperley	8. CONTRACT OR GRANT NUMBER(s)
9. PERFORMING ORGANIZATION NAME AND ADDRESS: US Army Ballistic Research Laboratory (ATTN: DRDAR-BLB) Aberdeen Proving Ground, MD 21005	10. PROGRAM ELEMENT, PROJECT, TASK AREA & WORK UNIT NUMBERS: 61101A/1T16110/A91A/00/ 015AJ
11. CONTROLLING OFFICE NAME AND ADDRESS: US Army Armament Research & Development Command, Ballistic Research Laboratory, ATTN: DRDAR-BL, Aberdeen Proving Ground, MD 21005 (11)	12. REPORT DATE: NOV[illegible] 1978
	13. NUMBER OF PAGES: 37
14. MONITORING AGENCY NAME & ADDRESS (if different from Controlling Office) (12) 37 p.	15. SECURITY CLASS. (of this report): Unclassified
	15a. DECLASSIFICATION/DOWNGRADING SCHEDULE

16. DISTRIBUTION STATEMENT (of this Report)

Approved for public release; distribution unlimited. (16) 1T161101A91A (17) 00

17. DISTRIBUTION STATEMENT (of the abstract entered in Block 20, if different from Report)

DDC RECEIVED JAN 19 1979 B

18. SUPPLEMENTARY NOTES

19. KEY WORDS (Continue on reverse side if necessary and identify by block number)

High-power electron accelerator
Transmission-line accelerator
Asymmetric transmission-line pairs
Reentrant transmission-line discontinuities
Laplace-transform analysis

20. ABSTRACT (Continue on reverse side if necessary and identify by block number) (idk)

A Laplace-transform analysis is presented of an equivalent circuit which represents a pair of asymmetric transmission lines coupled through a reentrant discontinuity. This cavity configuration is applicable for transmission-line accelerator designs. General expressions for the time-dependent open-circuit output voltage are derived. Some numerical examples for specific line geometries are presented.

DD FORM 1 JAN 73 1473 EDITION OF 1 NOV 65 IS OBSOLETE UNCLASSIFIED

393 471 SECURITY CLASSIFICATION OF THIS PAGE (When Data Entered)

TABLE OF CONTENTS

LIST OF FIGURES

1. INTRODUCTION

In two recent publications[1,2] we have presented a Laplace-transform analysis of charged transmission-line configurations for use in high-current particle accelerators. Two examples of constant-impedance cavity designs which could serve as the basic single stage in a multi-stage accelerator are shown in Fig. 1(a) and (b). In an internally-switched accelerator of this type the center electrode is first charged to some desired voltage with the switch system S in an open configuration. When the switches are subsequently closed, voltage pulses travel through the cavity, and the resulting voltage pattern at the output gap is dependent on the relative impedance of lines 1 and 2 which constitute the cavity line-pair and on the time elapsed from switch closure. If the passage of a pulsed electron beam down the beam pipe is appropriately timed with respect to the switch closure, the electron pulse will be accelerated when it passes the gap.

The equivalent circuit which was analyzed in References 1 and 2 to predict the general behavior of such accelerators is shown in Fig. 1(c). In the earlier reports we derived general expressions for the time-dependent open-circuit output voltage, the accelerating voltage per stage, and the conditions for maximum efficiency and maximum energy transfer to the beam load. It was shown that, in the lossless-line approximation, asymmetric line-pair configurations exist with which both a high accelerating voltage per stage and nominal unit efficiency can be achieved. A recirculating accelerator concept was also developed,[1] in which advantage is taken of a repetitive voltage waveform present in appropriately-designed transmission-line cavities to repeatedly accelerate a current pulse which is recirculated through the accelerator. It was shown that, with proper choice of parameters, this type of design again affords the possibility of nominal unit efficiency for energy transfer to the beam.

In the equivalent circuit of Fig. 1(c) no provision is made for treating the effect on the output voltage of the coupling region between lines 1 and 2. In Reference 1 a qualitative discussion of this effect was presented, in which the coupling region was treated as a shorted transmission line of impedance $Z_1 + Z_2$ (Z_1 and Z_2 being the characteristic impedances of lines 1 and 2, respectively) and electrical length Td, and a voltage step was traced through the system. The results of this analysis for two different asymmetric line-pair configurations are shown in Fig. 2, where we compare the open-circuit output voltage for d = 0.05ℓ

---

[1] *J.K. Temperley and D. Eccleshall, "Analysis of Transmission-Line Accelerator Concepts," Technical Report ARBRL-TR-02067, May 1978.* (AD #A056364)

[2] *D. Eccleshall and J.K. Temperley, "Transfer of Energy from Charged Transmission Lines with Applications to Pulsed High-Current Accelerators," J. Appl. Phys., Vol. 49, No. 7, pp. 3649-3655, July 1978.*

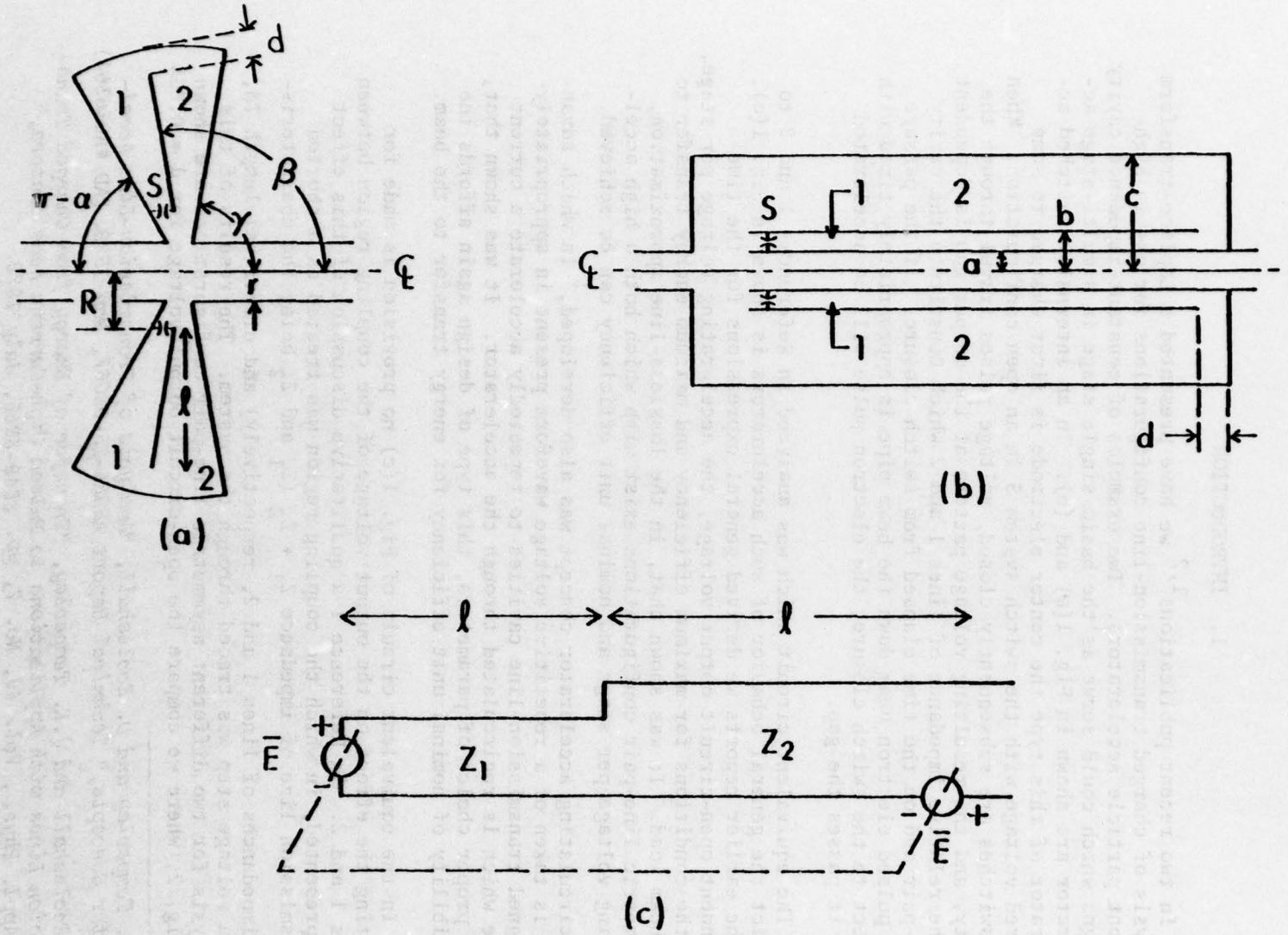

Figure 1. Transmission-line accelerator cavities. (a) Biconic radial lines. (b) Coaxial lines. (c) Equivalent circuit.

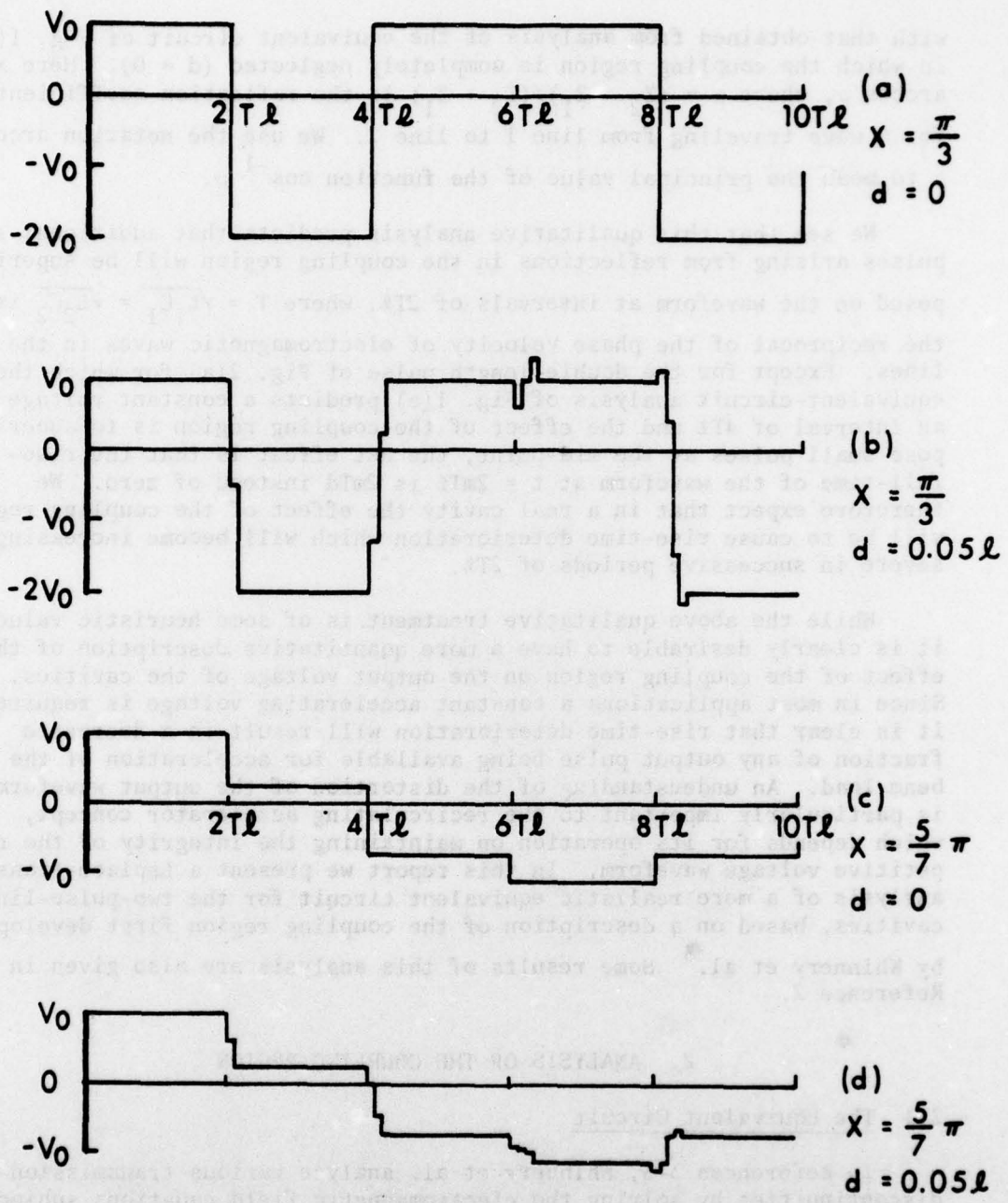

Figure 2. Idealized effect of coupling region on open-circuit output voltage. (a) $x = \frac{\pi}{3}$, coupling region neglected. (b) $x = \frac{\pi}{3}$, coupling region approximated by transmission line of length $d = 0.05\ell$. (c) $x = \frac{5}{7}\pi$, coupling region neglected. (d) $x = \frac{5}{7}\pi$, coupling region approximated by transmission line of length $d = 0.05\ell$.

with that obtained from analysis of the equivalent circuit of Fig. 1(c) in which the coupling region is completely neglected (d = 0). Here x = arccos ρ, where $\rho = (Z_2 - Z_1)/(Z_2 + Z_1)$ is the reflection coefficient for a wave traveling from line 1 to line 2. We use the notation arccos ρ to mean the principal value of the function $\cos^{-1} \rho$.

We see that this qualitative analysis predicts that additional short pulses arising from reflections in the coupling region will be superimposed on the waveform at intervals of $2T\ell$, where $T = \sqrt{L_1C_1} = \sqrt{L_2C_2}$ is the reciprocal of the phase velocity of electromagnetic waves in the lines. Except for the double-length pulse of Fig. 2(a) for which the equivalent-circuit analysis of Fig. 1(c) predicts a constant voltage for an interval of $4T\ell$ and the effect of the coupling region is to superimpose small pulses at the mid-point, the net effect is that the rise- or fall-time of the waveform at $t = 2mT\ell$ is $2mTd$ instead of zero. We therefore expect that in a real cavity the effect of the coupling region will be to cause rise-time deterioration which will become increasingly severe in successive periods of $2T\ell$.

While the above qualitative treatment is of some heuristic value, it is clearly desirable to have a more quantitative description of the effect of the coupling region on the output voltage of the cavities. Since in most applications a constant accelerating voltage is required, it is clear that rise-time deterioration will result in a decreased fraction of any output pulse being available for acceleration of the beam load. An understanding of the distortion of the output waveform is particularly important to the recirculating accelerator concept, which depends for its operation on maintaining the integrity of the repetitive voltage waveform. In this report we present a Laplace-transform analysis of a more realistic equivalent circuit for the two-pulse-line cavities, based on a description of the coupling region first developed by Whinnery et al.[3] Some results of this analysis are also given in Reference 2.

2. ANALYSIS OF THE COUPLING REGION

2.1 The Equivalent Circuit

In References 3-5, Whinnery et al. analyze various transmission-line discontinuities by solving the electromagnetic field equations subject

---

[3] *J.R. Whinnery and H.W. Jamieson, "Equivalent Circuits for Discontinuities in Transmission Lines," Proc. IRE 32, 98-115, 1944.*

[4] *J.R. Whinnery, H.W. Jamieson, and T.E. Robbins, "Coaxial-Line Discontinuities," Proc. IRE 32, 695-709, 1944.*

[5] *J.R. Whinnery and D.C. Stinson, "Radial Line Discontinuities," Proc. IRE 43, 46-51, 1955.*

to the geometry of the discontinuity. They show that a good approximation to the solutions of the field equations is obtained by inserting capacitive elements into the transmission-line equivalent circuit at the point of discontinuity and present graphs from which the appropriate values of the capacitance can be determined. For the simplest type of discontinuity, in which two transmission lines of similar geometry but different characteristic impedance are directly connected together, a single shunt capacitance is required at the discontinuity. For the reentrant type of discontinuity which occurs in the transmission-line accelerator cavities, the appropriate equivalent circuit is shown in Fig. 3. The three shunt capacitances occur also in the case of three transmission lines connected in series. The inductance arises from recognizing that a short transmission-line stub (the coupling region) has inductive character. The zero-impedance generators set up the initial conditions.

The values of L, C_1, C_2, and C_3 are determined by the detailed geometry of the transmission lines, in accordance with the solution of the field equations for any particular case. In all cases, however, C_3 is a negative number. To see that this is reasonable, we refer to Fig. 4. In Fig. 4(a) we show three coaxial lines connected in series. This will become the transmission-line cavity of Fig. 1(b) if line 3 is shorted. The three transmission lines of Fig. 4(a) can be transformed into a simple step discontinuity by shorting line 1, for example, as shown in Fig. 4(c). According to the analysis of Whinnery et al., the shunt capacitance C required for the equivalent circuit of Fig. 4(d) corresponding to the discontinuity of Fig. 4(c) is smaller than the capacitance C_2 which occurs in the equivalent circuit of Fig. 4(b) corresponding to the discontinuity of Fig. 4(a). Since to be consistent we must have $C = C_2 + C_3$, we see that C_3 must indeed have a negative value.

To provide results which have general validity, we will develop a Laplace-transfrom analysis of the circuit shown in Fig. 3, without making any assumptions about the geometry of the transmission lines. Some numerical examples for specific cases are presented in Section 3.

2.2 Previous Results

Before proceeding to the analysis of the coupling-region equivalent circuit, we collect here for ease of reference some of the results obtained in References 1 and 2 from the analysis of the equivalent circuit of Fig. 1(c). In that case we obtained for the transformed open-circuit output voltage

$$\bar{V} = \frac{V_0}{s} - \frac{2V_0\,(1+\rho)}{s}\,\frac{e^{-2sT\ell}}{1 + e^{-4sT\ell} + 2\rho\, e^{-2sT\ell}}, \qquad (1)$$

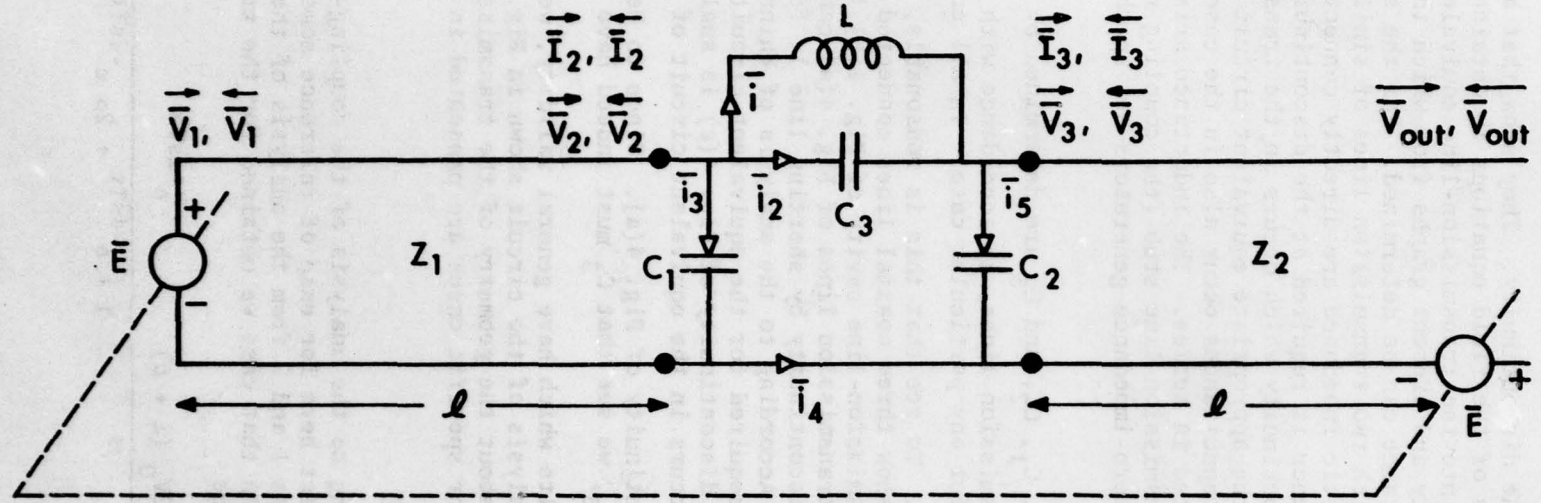

Figure 3. Equivalent circuit for transmission-line pair coupled through a reentrant discontinuity.

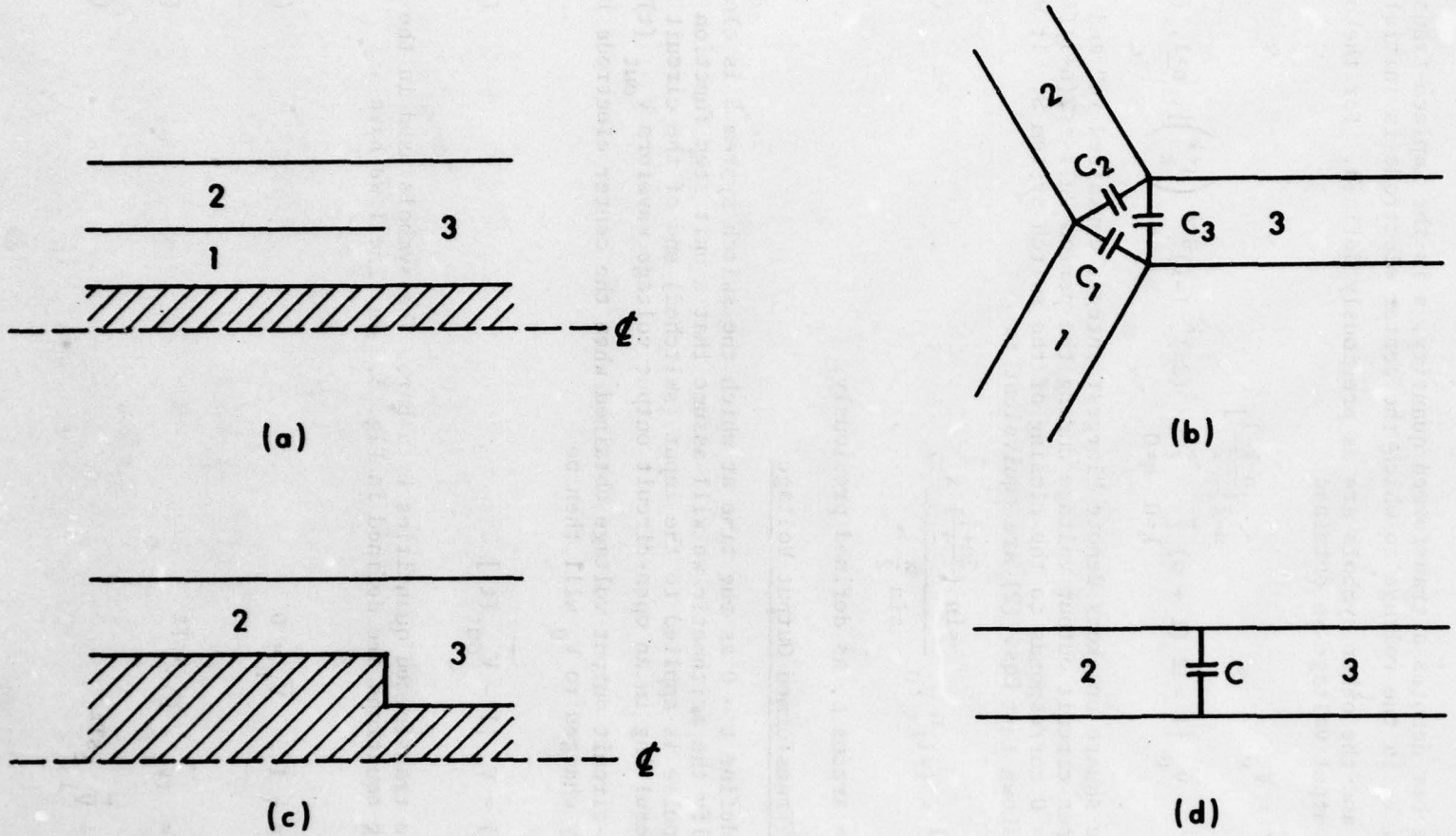

Figure 4. (a) Three coaxial lines in series. (b) Equivalent circuit for (a). (c) Step discontinuity formed from (a) by shorting line 1. (d) Equivalent circuit for (c).

where the bar denotes a transformed quantity, s is the Laplace-transform variable, V_0 is the voltage to which the center electrode is initially charged, and the other symbols are as previously defined. For the open-circuit output voltage we obtained

$$V^{(0)} = V_0$$

$$V^{(n)} = V_0 \left\{1 - 2\,(1+\rho) \sum_{k=0}^{n-1} \sum_{q=0}^{[\frac{n-k-1}{2}]} (2\rho)^k\, (-1)^{q+k} \binom{q+k}{k}\right\},\ n \geq 1, \quad (2)$$

where the square brackets denote "largest integer contained in" and $V^{(n)}$ is the open-circuit output voltage during the period $2nT\ell < t < 2(n+1)T\ell$, where $t = 0$ corresponds to the closing of the switch system S. It was further shown that Eqs. (2) are equivalent to

$$V^{(n)} = (-1)^n V_0 \frac{\sin\left(\frac{2n+1}{2}\right) x}{\sin \frac{x}{2}}\ , \quad (3)$$

where $x = \arccos \rho$, as defined previously.

2.3 The Transformed Output Voltage

We define $t = 0$ as the time at which the switch system S is closed. To simplify the arithmetic we will assume that a unit step function voltage pulse is applied to the input (switched) end of the circuit at $t = 0$, resulting in an open-circuit output voltage waveform $V_{out}(t)$. The open-circuit output voltage obtained when the center electrode is initially charged to V_0 will then be

$$V(t) = V_0\,[1 - V_{out}(t)]\ . \quad (4)$$

We denote transformed quantities by a bar. The symbols used in the following equations are defined in Fig. 3. In line 1 we have

$$\frac{\overrightarrow{\bar{V}}_1}{\overleftarrow{\bar{V}}_1} = -1\ , \quad \bar{V}_1 = 0 \quad (5)$$

$$\overrightarrow{\bar{V}}_2 = (\overrightarrow{\bar{V}}_1 + \bar{E})e^{-sT\ell} \quad (6)$$

$$\overleftarrow{\bar{V}}_2 = \overleftarrow{\bar{V}}_1\, e^{sT\ell} \quad (7)$$

$$\bar{V}_2 = \vec{\bar{V}}_2 + \overleftarrow{\bar{V}}_2 \tag{8}$$

$$\bar{I}_2 = \vec{\bar{I}}_2 + \overleftarrow{\bar{I}}_2 \tag{9}$$

$$\frac{\vec{\bar{V}}_2}{\vec{\bar{I}}_2} = Z_1 = -\frac{\overleftarrow{\bar{V}}_2}{\overleftarrow{\bar{I}}_2} . \tag{10}$$

These can be combined to yield

$$\bar{I}_2 = \frac{\vec{\bar{V}}_2}{Z_1} - \frac{\overleftarrow{\bar{V}}_2}{Z_1}$$

$$= \frac{1}{Z_1} \frac{\bar{V}_2 \ (1 + e^{2sT\ell}) - 2(\bar{E}) e^{sT\ell}}{1 - e^{2sT\ell}} . \tag{11}$$

Similarly in line 2

$$\frac{\vec{\bar{V}}_{out}}{\overleftarrow{\bar{V}}_{out}} = 1 \ , \ \bar{V}_{out} = 2\,\vec{\bar{V}}_{out} = 2\,\overleftarrow{\bar{V}}_{out} \tag{12}$$

$$\vec{\bar{V}}_3 = \vec{\bar{V}}_{out}\, e^{sT\ell} \tag{13}$$

$$\overleftarrow{\bar{V}}_3 = \overleftarrow{\bar{V}}_{out}\, e^{-sT\ell} \tag{14}$$

$$\bar{V}_3 = \vec{\bar{V}}_3 + \overleftarrow{\bar{V}}_3 \tag{15}$$

$$\bar{I}_3 = \vec{\bar{I}}_3 + \overleftarrow{\bar{I}}_3 \tag{16}$$

$$\frac{\vec{\bar{V}}_2}{\vec{\bar{I}}_2} = Z_2 = -\frac{\overleftarrow{\bar{V}}_2}{\overleftarrow{\bar{I}}_2} . \tag{17}$$

From equations (12)-(17) we obtain

$$\bar{I}_3 = \frac{\bar{V}_{out}}{Z_2} \sinh sT\ell \tag{18}$$

and

$$\bar{V}_3 = \bar{V}_{out} \cosh sT\ell \ . \tag{19}$$

We have further

$$\begin{aligned} \bar{I}_2 &= \bar{i}_1 + \bar{i}_2 + \bar{i}_3 \ , \\ \bar{V}_2 &= \frac{\bar{i}_3}{sC_1} \ , \\ \bar{V}_2 - \bar{V}_3 &= \frac{\bar{i}_2}{sC_3} \ , \\ \bar{V}_2 - \bar{V}_3 &= \bar{i}_1 \, sL \ , \end{aligned} \tag{20}$$

so that

$$\begin{aligned} \bar{I}_2 &= \frac{\bar{V}_2 - \bar{V}_3}{sL} + (\bar{V}_2 - \bar{V}_3) sC_3 + \bar{V}_2 \, sC_1 \\ &= \bar{V}_2 \left(\frac{1}{sL} + sC_3 + sC_1\right) - \bar{V}_2 \left(\frac{1}{sL} + sC_3\right) \ . \end{aligned} \tag{21}$$

Equating equations (21) and (11) gives

$$\begin{aligned} &\bar{V}_2 \left(\frac{\coth sT\ell}{Z_1} + \frac{1}{sL} + sC_3 + sC_1\right) \\ &\quad = \bar{V}_3 \left(\frac{1}{sL} + sC_3\right) + \frac{\bar{E}}{Z_1 \sinh sT\ell} \ . \end{aligned} \tag{22}$$

Substituting (19) into (22) yields

$$\bar{V}_2 \left(\frac{\coth s\tau\ell}{Z_1} + \frac{1}{sL} + sC_3 + sC_1\right) = \bar{V}_{out} \left(\frac{1}{sL} + sC_3\right) \cosh s\tau\ell + \frac{\bar{E}}{Z_1 \sinh s\tau\ell} \quad . \tag{23}$$

Now also

$$\bar{I}_2 = \bar{i}_3 - \bar{i}_4 \quad ,$$

$$\bar{I}_3 = \bar{i}_1 + \bar{I}_2 - \bar{I}_5 \quad , \tag{24}$$

$$\bar{V}_3 = \frac{\bar{I}_5}{sC_2} \quad ,$$

$$\bar{V}_2 - \bar{V}_3 = \frac{\bar{I}_2}{sC_3} \quad ,$$

which give

$$\bar{I}_3 = \frac{\bar{V}_2 - \bar{V}_3}{sL} + (\bar{V}_2 - \bar{V}_3)sC_3 - sC_2 \bar{V}_3 \quad . \tag{25}$$

Equating (18) and (25) yields

$$\frac{\bar{V}_{out}}{Z_2} \sinh s\tau\ell = \frac{\bar{V}_2 - \bar{V}_3}{sL} + (\bar{V}_2 - \bar{V}_3)\, sC_3 - sC_2 \bar{V}_3 \quad . \tag{26}$$

Substituting for $\bar{V}_3$ from (19) gives

$$\bar{V}_{out} \left[\frac{\sinh s\tau\ell}{Z_2} + \left(\frac{1}{sL} + sC_3 + sC_2\right) \cosh s\tau\ell\right] = \bar{V}_2 \left(\frac{1}{sL} + sC_3\right). \tag{27}$$

Equations (23) and (27) then imply

$$\bar{V}_{out} \left\{\frac{\cosh s\tau\ell}{Z_1 Z_2} + \frac{1}{Z_2}\left(\frac{1}{sL} + sC_3 + sC_1\right) \sinh s\tau\ell + \frac{1}{Z_1}\left(\frac{1}{sL} + sC_3 + sC_2\right) \frac{\cosh^2 s\tau\ell}{\sinh s\tau\ell} + \left(\frac{1}{sL} + sC_3 + sC_1\right)\left(\frac{1}{sL} + sC_3 + sC_2\right) \cosh s\tau\ell - \left(\frac{1}{sL} + sC_3\right)^2 \cosh s\tau\ell\right\}$$

$$= \frac{\left(\frac{1}{sL} + sC_3\right)}{s\, Z_1 \sinh s\tau\ell} \quad , \tag{28}$$

where we have put $\bar{E} = \frac{1}{s}$. Equation (28) can be put into the form

$$\bar{V}_{out} = \frac{4Z_2(1 + s^2 LC_3)}{s\alpha(s)} \frac{e^{-2st\ell}}{1 + \frac{\gamma(s)}{\alpha(s)} e^{-2sT\ell} + \frac{\beta(s)}{\alpha(s)} e^{-4sT\ell}} , \tag{29}$$

where

$$\begin{aligned} \alpha(s) &= Z_1 + Z_2 + s\,[L + Z_1 Z_2 (C_1 + C_2)] \\ &\quad + s^2 L\,[Z_1 (C_3 + C_1) + Z_2 (C_3 + C_2)] \\ &\quad + s^3 Z_1 Z_2 L (C_1 C_2 + C_1 C_3 + C_2 C_3) , \end{aligned} \tag{30}$$

$$\begin{aligned} \beta(s) &= Z_1 + Z_2 - s\,[L + Z_1 Z_2 (C_1 + C_2)] \\ &\quad + s^2 L\,[Z_1 (C_3 + C_1) + Z_2 (C_3 + C_2)] \\ &\quad - s^3 Z_1 Z_2 L (C_1 C_2 + C_1 C_3 + C_2 C_3) , \end{aligned}$$

and $\gamma(s) = 2\{Z_2 - Z_1 - s^2 L\,[Z_1 (C_3 + C_1) - Z_2 (C_3 + C_2)]\}$.

We note that if $L = C_1 = C_2 = C_3 = 0$ we obtain

$$\begin{aligned} \bar{V}_{out} &= \frac{4Z_2}{s\,(Z_1 + Z_2)} \frac{e^{-2sT\ell}}{1 + 2\frac{(Z_2 - Z_1)}{Z_2 + Z_1} e^{-2sT\ell} + e^{-4sT\ell}} \\ &= \frac{2\,(1 + \rho)}{s} \frac{e^{-2sT\ell}}{1 + e^{-4sT\ell} + 2\rho e^{-2sT\ell}} . \end{aligned} \tag{31}$$

Since from (4) by definition

$$\bar{V} = V_0\,(\tfrac{1}{s} - \bar{V}_{out}) ,$$

we have

$$\bar{V} = \frac{V_0}{s} - \frac{2V_0\,(1 + \rho)}{s} \frac{e^{-2sT\ell}}{1 + e^{-4sT\ell} + 2\rho e^{-2sT\ell}} . \tag{32}$$

Equation (32) is identical to the expression (1) which we obtained earlier[1,2] in our analysis of the equivalent circuit neglecting the coupling region.

2.4 The Inverse Transform

We define

$$S_{2k}(t) = \begin{cases} 0, & t < 2kT\ell \\ 1, & t > 2kT\ell \end{cases},$$

$$D(s) = \alpha(s) + \gamma(s)\, e^{-2sT\ell} + \beta(s)\, e^{-4sT\ell}, \tag{33}$$

$$D^{(1)}(s_n) = \frac{d}{ds} D(s)\Big|_{s = s_n},$$

where the s_n are the solutions of

$$D(s) = 0.$$

Then the formal inverse transform of (29) is

$$V_{out} = S_2(t)\left\{1 + 4Z_2 \sum_{s_n} \frac{(1 + s_n^2 LC_3)e^{s_n(t - 2T\ell)}}{D^{(1)}(s_n)}\right\}, \tag{34}$$

where we have assumed that the s_n are all distinct. While equation (34) could be useful in numerical solutions of specific problems, it is not very helpful in trying to visualize the output waveform. In particular, except for the explicit step at $t = 2T\ell$, it does not display the inherent periodicity of the output voltage which is evident in equations (2) and (3). We will therefore pursue a development analogous to that leading to equation (2) in order to derive a more illuminating (but more complicated-appearing) expression for the open-circuit output voltage.

We expand the denominator of the second factor of equation (29) in a binomial series to obtain

$$V_{out} = \frac{4Z_2(1 + s^2 LC_3)e^{-2sT\ell}}{s\alpha(s)} \sum_{n=0}^{\infty} (-1)^n \left\{\frac{\gamma(s)}{\alpha(s)} e^{-2sT\ell} + \frac{\beta(s)}{\alpha(s)} e^{-4sT\ell}\right\}^n. \tag{35}$$

A further expansion of the summand in equation (35) yields

$$V_{out} = \frac{4Z_2\,(1 + s^2\,LC_3)}{s} \sum_{n=0}^{\infty} \frac{(-1)^n}{[\alpha(s)]^{n+1}} \sum_{k=0}^{n} \binom{n}{k} e^{-2(2n - k + 1)sT\ell} \times [\beta(s)]^{n-k}\,[\gamma(s)]^k \quad . \tag{36}$$

We now write

$$\alpha(s) = \alpha_1\,s^3 + \alpha_2\,s^2 + \alpha_3\,s + \alpha_4 \tag{37}$$

and define

$$A(s) = \frac{\alpha(s)}{\alpha_1} \quad . \tag{38}$$

Let the roots of $A(s) = 0$ be a_1, a_2, a_3. In the following we assume these are distinct. Then equation (36) becomes

$$\overline{V}_{out} = 4Z_2 \sum_{n=0}^{\infty} \sum_{k=0}^{n} (-1)^n \binom{n}{k} \frac{(1 + s^2LC_3)[\beta(s)]^{n-k}[\gamma(s)]^k e^{-2(2n-k+1)sT\ell}}{\alpha_1^{n+1} s(s-a_1)^{n+1}(s-a_2)^{n+1}(s-a_3)^{n+1}} \quad . \tag{39}$$

We define $f(s)$ by writing (39) as

$$\overline{V}_{out} = 4Z_2 \sum_{n=0}^{\infty} \sum_{k=0}^{n} (-1)^n \binom{n}{k} \frac{1}{\alpha_1^{n+1}} f(s) e^{-2(2n-k+1)sT\ell} \quad . \tag{40}$$

The inverse transform is

$$V_{out}(t) = 4Z_2 \sum_{n=0}^{\infty} \sum_{k=0}^{n} (-1)^n \binom{n}{k} \frac{1}{\alpha_1^{n+1}} S_{2(2n-k+1)}(t)\; F(t-2(2n-k+1)T\ell), \tag{44}$$

where

$$F(t) \equiv L^{-1}\{f(s)\} \quad .$$

Now

$$L^{-1}\{f(s)\} = \sum_j R_j(t) ,$$

where $R_j(t)$ is the residue of $e^{zt} f(z)$ at the j^{th} pole. The function $f(s)$ has a simple pole at $s = 0$ and poles of order $n+1$ at $s = a_1, a_2, a_3$. Hence

$$L^{-1}\{f(s)\} = \frac{[\beta(0)]^{n-k}[\gamma(0)]^k}{(-a_1a_2a_3)^{n+1}} + \sum_{j=1}^{3} e^{a_j t} \sum_{r=0}^{n} \frac{t^r}{r!} A_{-(r+1),j} , \qquad (42)$$

where

$$A_{-(r+1),j} = \frac{1}{(n-r)!} \frac{d^{n-r}}{d\, s^{n-r}} (s-a_j)^{n+1} f(s)\Big|_{s = aj} .$$

We now define

$$(s-a_j)^{n+1} f(s) = \frac{u_{n,k}(s)}{s} . \qquad (43)$$

so that

$$u_{n,k}(s) = \frac{(1 + s^2 LC_3)[\beta(s)]^{n-k}[\gamma(s)]^k}{\prod_{\substack{i=1 \\ i\neq j}}^{3} (s-a_i)^{n+1}} . \qquad (44)$$

We note that

$$\frac{d^{n-r}}{ds^{n-r}}\left[\frac{u_{n,k(s)}}{s}\right] = \sum_{p=0}^{n-r} \binom{n-r}{p} [u^{(n-r-p)}(s)] \frac{(-1)^p p!}{s^{p+1}} , \qquad (45)$$

where we have used the notation

$$u^{(k)}(s) = \frac{d^k u(s)}{ds^k} .$$

Using equation (45), and with some manipulation of the indices of summation, equation (42) can be written

$$L^{-1}\{f(s)\} = \frac{[\beta(0)]^{n-k}[\gamma(0)]^k}{(-a_1a_2a_3)^{n+1}} +$$

$$+ \sum_{j=1}^{3} e^{a_j t} \sum_{r=0}^{n} \frac{(-1)^r t^{n-r}}{(n-r)!\, a_j^r} \sum_{p=0}^{r} \frac{(-1)^p a_j^{(p-1)}}{p!} u_{n,k}^{(p)}(a_j) \quad . \qquad (46)$$

Hence from (41) we obtain

$$V_{out}(t) = 4Z_2 \sum_{n=0}^{\infty} \sum_{k=0}^{n} (-1)^n \binom{n}{k} \frac{1}{\alpha_1^{n+1}} S_{2(2n-k+1)}(t)$$

$$x \left\{ \frac{[\beta(0)]^{n-k}[\gamma(0)]^k}{(-a_1 a_2 a_3)^{n+1}} + \sum_{j=1}^{3} e^{a_j[t-2(2n-k+1)T\ell]} \right.$$

$$\left. x \sum_{r=0}^{n} \frac{(-1)^r [t-2(2n-k+1)T\ell]^{n-r}}{(n-r)!\, a_j^r} \sum_{p=0}^{r} \frac{(-1)^p a_j^{p-1}}{p!} u_{n,k}^{(p)}(a_j) \right\} . \quad (47)$$

We now wish to change from summations on n and k to summations on m and k, where m = 2n-k. To do this we note the correspondences:

m	n	k
0	0	0
1	1	1
2	1	0
2	2	2
3	2	1
3	3	3
4	2	0
4	3	2
4	4	4
5	3	1
5	4	3
5	5	5
6	3	0
6	4	2
6	5	4
6	6	6

We note that for each even (odd) value of m, k takes on all even (odd) values from 0 to m. Hence equation (47) becomes

$$V_{out} = 4Z_2 \sum_{\substack{m=0 \\ m \text{ even}}}^{\infty} \sum_{\substack{k=0 \\ k \text{ even}}}^{m} (-1)^{\frac{m+k}{2}} \binom{\frac{m+k}{2}}{k} \frac{S_{2(m+1)}(t)}{\alpha_1^{\frac{m+k+2}{2}}}$$

$$\times \left\{ \frac{[\beta(0)]^{\frac{m-k}{2}} [\gamma(0)]^k}{(-a_1 a_2 a_3)^{\frac{m+k+2}{2}}} + \sum_{j=1}^{3} e^{a_j[t-2(m+1)T\ell]} \right.$$

$$\left. \times \sum_{r=0}^{\frac{m+k}{2}} \frac{(-1)^r [t-2(m+1)T\ell]^{\frac{m+k}{2}-r}}{(\frac{m+k}{2}-r)!\, a_j^r} \sum_{p=0}^{r} \frac{(-1)^p a_j^{p-1}}{p!} u^{(p)}_{\frac{m+k}{2},\, k}(a_j) \right\}$$

$$+ 4Z_2 \sum_{\substack{m=0 \\ m \text{ odd}}}^{\infty} \sum_{\substack{k=0 \\ k \text{ odd}}}^{m} (\text{same thing}). \qquad (48)$$

We now define

$$V^{(n)}_{out} = V^{(n)}(t),\ 2nT\ell<t<2(n+1)T\ell,\ n\geq 1\ , \qquad (49)$$

and using the properties of the step function $S_k(t)$ we obtain from (48)

$$V^{(n)}_{out} = 4Z_2 \sum_{\substack{m=0 \\ m \text{ even}}}^{n-1} \sum_{\substack{k=0 \\ k \text{ even}}}^{m} (-1)^{\frac{m+k}{2}} \binom{\frac{m+k}{2}}{k} \frac{1}{\alpha_1^{\frac{m+k+2}{2}}}$$

$$\times \left\{ \frac{[\beta(0)]^{\frac{m-k}{2}} [\gamma(0)]^k}{(-a_1 a_2 a_3)^{\frac{m+k+2}{2}}} + \sum_{j=1}^{3} e^{a_j[t-2(m+1)T\ell]} \right.$$

$$\left. \times \sum_{r=0}^{\frac{m+k+2}{2}} \frac{(-1)^r [t-2(m+1)T\ell]^{\frac{m+k}{2}-r}}{(\frac{m+k}{2}-r)!\, a_j^r} \sum_{p=0}^{r} \frac{(-1)^p a_j^{p-1}}{p!} u^{(s)}_{\frac{m+k}{2},\, k}(a_j) \right\}$$

$$+ 4Z_2 \sum_{\substack{m=0 \\ m \text{ odd}}}^{n-1} \sum_{\substack{k=0 \\ k \text{ odd}}}^{m} (\text{same thing}). \qquad (50)$$

We define $\sigma(m,k)$ by writing (50) in the form

$$V_{out}^{(n)} = 4Z_2 \sum_{\substack{m=0 \\ m \text{ even}}}^{n-1} \sum_{\substack{k=0 \\ k \text{ even}}}^{m} \sigma(m,k) + 4Z_2 \sum_{\substack{m=0 \\ m \text{ odd}}}^{n-1} \sum_{\substack{k=0 \\ k \text{ odd}}}^{m} \sigma(m,k) \quad . \qquad (51)$$

We now wish to interchange the order of summation on m and k and replace m by $q = \frac{m-k}{2}$. This is facilitated by noting the correspondences of the following table:

k	m	q
n-1	n-1	0
n-2	n-2	0
n-3	n-3	0
	n-1	1
n-4	n-4	0
	n-2	1
n-5	n-5	0
	n-3	1
	n-1	2

We see that for each value of k we have $0 \leq q \leq [\frac{n-1-k}{2}]$, where the square brackets denote "largest integer contained in." Then eq. (51) becomes

$$V_{out}^{(n)} = 4Z_2 \sum_{\substack{m=0 \\ m \text{ even}}}^{n-1} \sum_{q=0}^{[\frac{n-1-k}{2}]} \sigma(2q+k,k) + 4Z_2 \sum_{\substack{m=0 \\ m \text{ odd}}}^{n-1} \sum_{q=0}^{[\frac{n-1-k}{2}]} \sigma(2q+k,k)$$

$$= 4Z_2 \sum_{m=0}^{n-1} \sum_{q=0}^{[\frac{n-1-k}{2}]} \sigma(2q+k,k) \quad . \qquad (52)$$

Hence, using (4), we obtain for the open-circuit output voltage

$$V^{(0)} = V_0 \quad ,$$

$$V^{(n)} = V_0 - 4V_0 Z_2 \sum_{k=0}^{n-1} \sum_{q=0}^{[\frac{n-1-k}{2}]} \frac{(-1)^{q+k}}{\alpha_1^{q+k+1}} \binom{q+k}{k} \frac{[\beta(Q)]^q [\gamma(Q)]^k}{(-a_1 a_2 a_3)^{q+k+1}} +$$

$$- 4V_0 Z_2 \sum_{k=0}^{n-1} \sum_{q=0}^{[\frac{n-1-k}{2}]} \frac{(-1)^{q+k}}{\alpha_1^{q+k+1}} \binom{q+k}{k} \sum_{j=1}^{3} e^{a_j[t-2(2q+k+1)T\ell]}$$

$$\times \sum_{r=0}^{q+k} \frac{(-1)^r [t-2(2q+k+1)T\ell]^{q+k-r}}{(q+k-r)!\, a_j^r} \sum_{p=0}^{r} \frac{(-1)^p a_j^{p-1}}{p!} u^{(p)}_{q+k,k}(a_j), \quad n \geq 1. \quad (53)$$

We now define $U^{(n)}$ to be the terms in (53) which do not contain explicit time dependence. We have

$$U^{(n)} = V_0 \left\{ 1 - 4Z_2 \sum_{k=0}^{n-1} \sum_{q=0}^{[\frac{n-k-1}{2}]} \frac{(-1)^{q+k}}{\alpha_1^{q+k+1}} \binom{q+k}{k} \frac{[\beta(0)]^q [\gamma(0)]^k}{(-a_1 a_2 a_3)^{q+k+1}} \right\}. \quad (54)$$

But from equations (37) and (38) and the definition of a_1, a_2, a_3, we find

$$\alpha_1 (-a_1 a_2 a_3) = \alpha_1 \left(\frac{\alpha_4}{\alpha_1}\right) = \alpha_4 .$$

Referring to the defining equations (30) we find

$$\alpha_4 = Z_1 + Z_2 ,$$

$$\beta(0) = Z_1 + Z_2 ,$$

$$\gamma(0) = 2(Z_2 - Z_1) .$$

Hence (54) becomes

$$U^{(n)} = V_0 \left\{ 1 - \frac{4Z_2}{Z_2+Z_1} \sum_{k=0}^{n-1} \sum_{q=0}^{[\frac{n-k-1}{2}]} (-1)^{q+k} \binom{q+k}{k} 2^k \frac{(Z_2-Z_1)^k}{(Z_2+Z_1)^k} \right\}$$

$$= V_0 \left\{ 1 - 2(1+\rho) \sum_{k=0}^{n-1} \sum_{q=0}^{[\frac{n-k-1}{2}]} (-1)^{q+k} \binom{q+k}{k} (2\rho)^k \right\}. \quad (55)$$

Comparing (55) with (2), we see that $U^{(n)}$ is just the open-circuit output voltage that is obtained when the coupling region is ignored. The remaining terms in (53) represent the perturbation on the output voltage produced by the finite coupling region.

We see by inspection that equation (53) has the form

$$V^{(n)} = U^{(n)} - V_0 \sum_{j=1}^{3} \sum_{m=1}^{n} e^{a_j(t-2mT\ell)} P_{j,m-1}(t-2mT\ell) , \qquad (56)$$

where $P_{j,m-1}(t)$ is a polynomial of degree (m-1) in t. The coefficients of the powers of $(t-2mT\ell)$ in $P_{j,m-1}$ are dependent on the a_j (and hence on the values of the equivalent-circuit parameters), but are just numbers independent of t. Physically it is clear that the a_j must be negative real numbers or complex numbers with negative real parts. The perturbation therefore consists of a sum of decaying exponentials or a sum of exponentially decaying oscillations. These are, however, multiplied by polynomials whose degree becomes higher in succeeding periods of $2T\ell$. Hence the perturbation term will approach zero more slowly in later pulses than in earlier ones, and the rise-time deterioration will become increasingly severe. This agrees with our earlier qualitative treatment. Clearly an optimum design would have $-Re(a_j)$ as large as possible, so that each additional perturbation occurring at the beginning a period of $2T\ell$ would damp out shortly after $t = 2nT\ell$. If this can be achieved the perturbations will not "carry over" from one pulse to the next until n becomes large. Unfortunately, the arithmetic of the preceding analysis is too complicated to permit a quantitative statement of this criterion.

3. Some Numerical Examples

In this section we present for several specific transmission-line configurations the output-voltage waveforms for the period $0<t<4T\ell$ as obtained from expression (53). In all cases we of course have $V^{(0)} = V_0$. For the pulse $V^{(1)}$ we obtain

$$V^{(1)} = V_0 \{1 - 2(1+\rho)\} - \frac{4V_0Z_2}{\alpha_1} \left\{ \frac{(1 + a_1^2 LC_3)e^{a_1\tau}}{a_1(a_1 - a_2)(a_1 - a_3)} \right.$$

$$\left. + \frac{(1 + a_2^2 LC_3)e^{a_2\tau}}{a_2(a_2 - a_1)(a_2 - a_3)} + \frac{(1 + a_3^2 LC_3)e^{a_3\tau}}{a_3(a_3 - a_1)(a_3 - a_2)} \right\} , \qquad (57)$$

where $\tau = t - 2T\ell$, and the other symbols are as previously defined. The values of the equivalent-circuit parameters will be obtained from References 3-5. It is important to recognize, however, that these are valid

only for electromagnetic wavelengths which are greater than twice the largest transverse dimension of the system. Hence care must be exercised in interpreting the leading portion of pulsed waveforms which may be dominated by high-frequency components of the pulse. The results are expected to be valid for $\tau > \tau_{min}$, where τ_{min} is given by $\tau_{min} \simeq w/2v$, with w the largest transverse dimension of the line-pair system and v the phase velocity of electromagnetic waves in the lines.

We take as our first example a symmetric strip-line pair with $Z_1 = Z_2 = 50\ \Omega$ and vacuum dielectric. In the notation of Fig. 5(a) the dimensions are a = 2.92 cm, d = 11.1 cm, x = 0.0127 cm, ℓ = 305 cm, and the width of the lines is 15.24 cm. From Reference 3 we then find

$$C_1 = C_2 = 0.83 \text{ pf}$$

$$C_3 = -0.4 \text{ pf}$$

$$L = 53.5 \text{ nh.}$$

Expression (38) for this case is

$$A(s) = s^3 + 24.6 \times 10^{10}\, s^2 + 57.7 \times 10^{20}\, s + 10 \times 10^{30}$$

and the roots of A(s) are

$$a_1 = -0.189 \times 10^{10}$$

$$a_2 = -2.4 \times 10^{10}$$

$$a_3 = -22. \times 10^{10} \quad .$$

From (57) we then obtain, with τ expressed in nanoseconds,

$$V^{(1)} = V_0 - V_0 \left\{2 - 2.04e^{-1.89\tau} - 2e^{-24\tau} + 2.04e^{-220\tau}\right\} \quad .$$

This result is plotted in Figure 5(b). We see that $V^{(1)}$ reaches 90% of its final value of $-V_0$ at τ = 1.5 ns. The sharp spike which occurs between $\tau = 0$ and $\tau = \tau_{min}$ is a result of the inadequacy of the equivalent-circuit treatment at very early times.

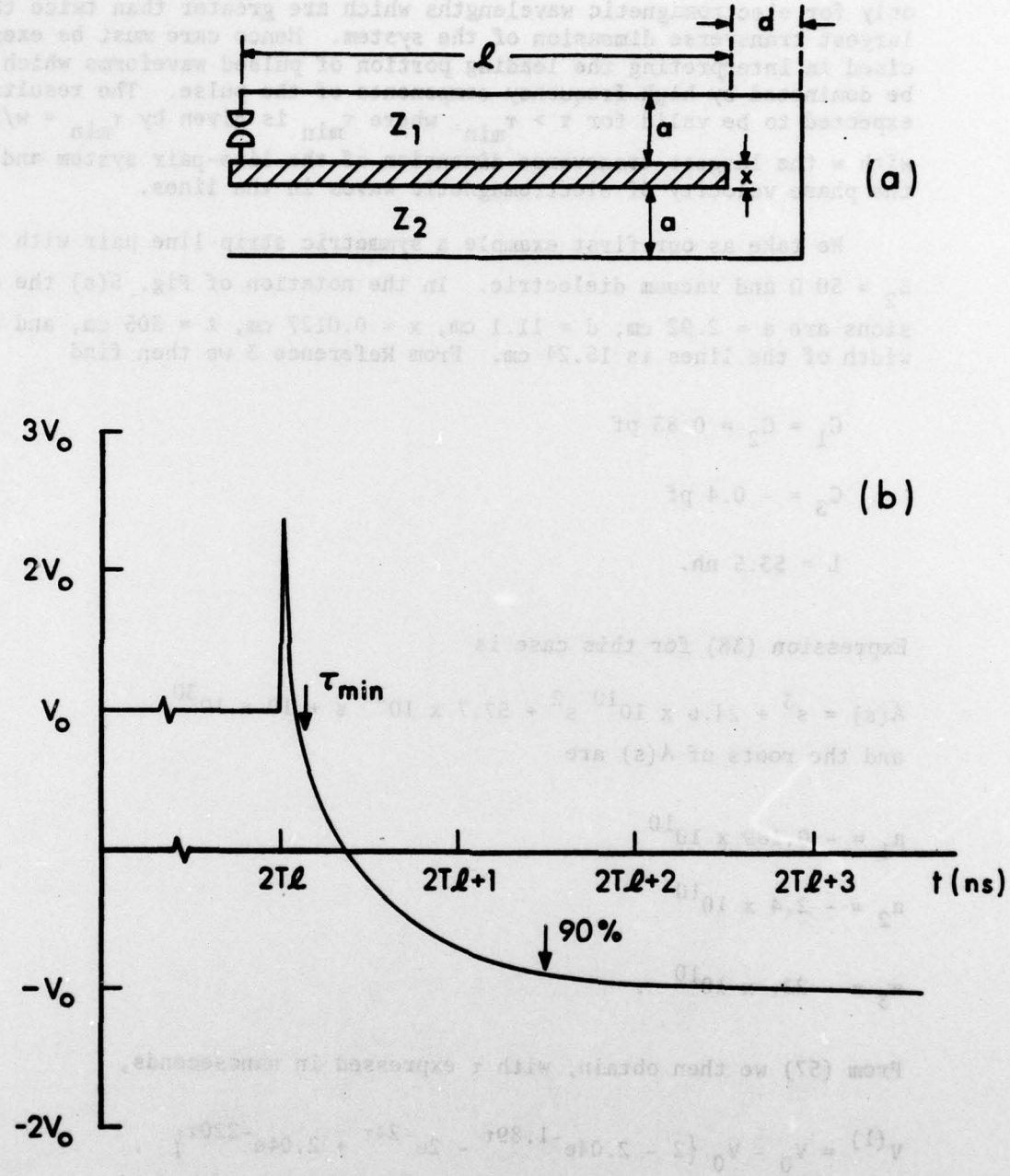

Figure 5. (a) Symmetric strip-line pair. (b) Open-circuit output pulse $V^{(1)}$.

This case has been studied experimentally using copper strips having the dimensions treated here.[6] The input pulse had a risetime of 1.1 ns, and the risetime degradation observed in the output pulse was completely consistent with the analytical result shown in Figure 5(b) for $\tau > \tau_{min}$.

As a second example we choose an asymmetric cylindrical coaxial line pair with $Z_1 = 20.2\ \Omega$, $Z_2 = 61.7\ \Omega$, and vacuum dielectric. In the notation of Fig. 6(a) the dimensions are $r_1 = 5$ cm, $r_2 = 14$ cm, $r_3 = 21$ cm, $x = 1$ cm, $\ell = 160$ cm, and $d = 6$ cm. The equivalent-circuit parameters are to be taken from Reference 4. This reference does not treat the effect of finite thickness of the intermediate electrode. By analogy with the treatment in Reference 3 for strip lines, however, we find that the values of C_3 obtained from Reference 4 should be multiplied by 1.2, and the values of C_1 and C_2 by 1.06. The re-entrant discontinuity is also not treated explicitly in Reference 4, but again by analogy with Reference 3 we find that the capacitances are the same as for three transmission lines in series (Figure 4(a)), and the inductance is obtained by multiplying the inductance per unit length of the coupling region by its length. Correction of the values of the capacitances is required because of the termination of the coupling region close to the discontinuity. From Figure 18 of Reference 3 and Figure 14 of Reference 4 we can infer that this requires multiplication of the capacitances by an additional factor of 1.2. We then obtain

$$C_1 = 8.2 \text{ pf}$$

$$C_2 = 2.8 \text{ pf}$$

$$C_3 = -1.9 \text{ pf}$$

$$L = 17.2 \text{ nh.}$$

Expression (38) for this case is

$$A(s) = s^3 + 7.12 \times 10^{10}\, s^2 + 7.00 \times 10^{20}\, s + 1.85 \times 10^{30}$$

and the roots of $A(s) = 0$ are

---

[6] *C.E. Hollandsworth, BRL Report (to be published).*

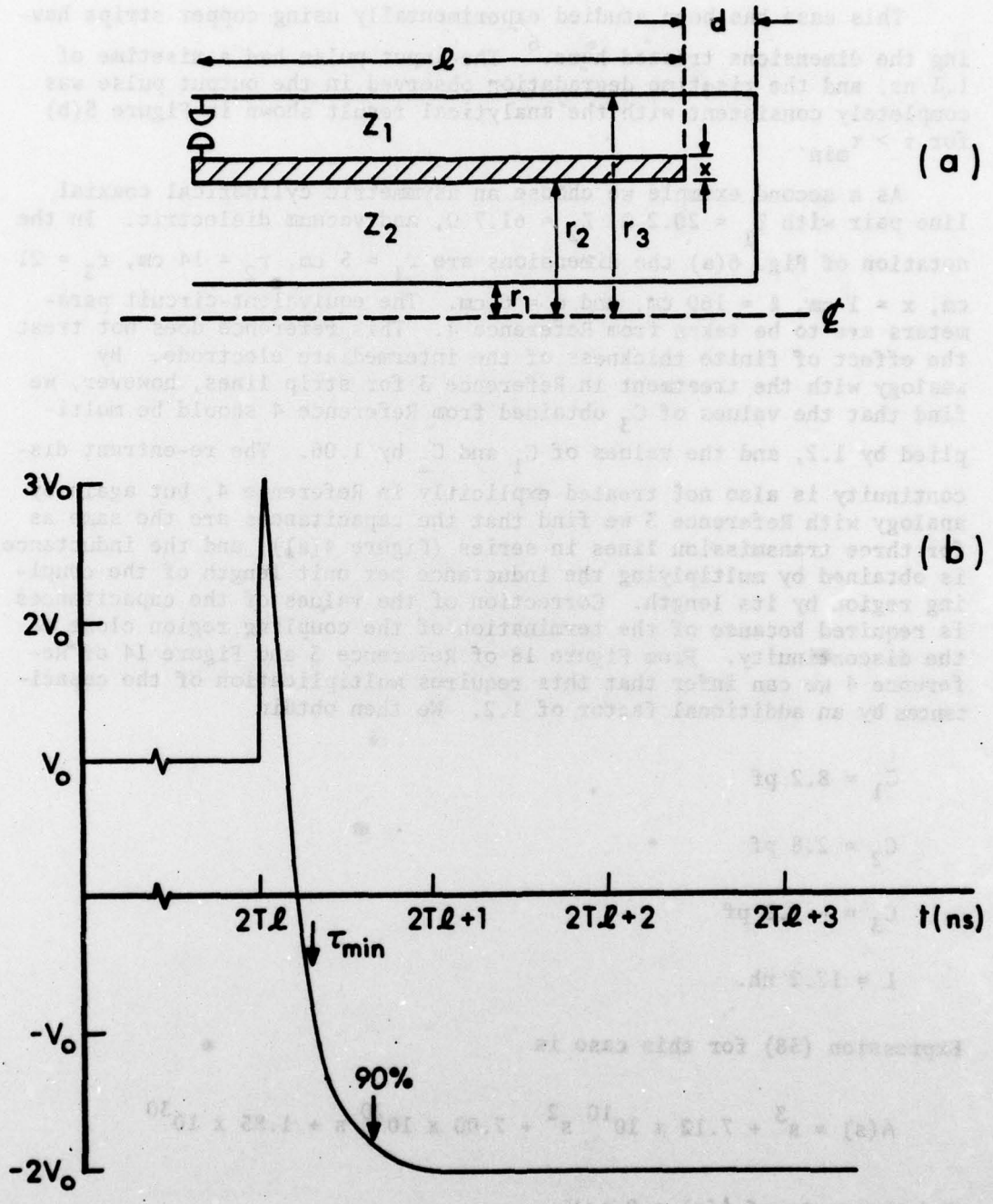

Figure 6. (a) Asymmetric coaxial-line pair. (b) Open-circuit output pulse $V^{(1)}$.

$$a_1 = -0.509 \times 10^{10}$$

$$a_2 = -0.606 \times 10^{10}$$

$$a_3 = -6.01 \times 10^{10} .$$

From (57) we obtain, with τ in nanoseconds,

$$V^{(1)} = V_0 - V_0 \{3.01 - 3.15e^{-5.09\tau} - 3.52e^{-6.06\tau} + 3.66e^{-60.1\tau}\} .$$

This result is plotted in Figure 6(b). The output pulse $V^{(1)}$ reaches 90% of its final value of $-2V_0$ in 0.65 ns. Again expression (57) results in a non-physical spike ocurring between $\tau = 0$ and $\tau = \tau_{min}$.

This line-pair geometry has been studied with a computer code which calculates the electric and magnetic field strengths as a function of time for electromagnetic waves traveling in cavity structures.[7] Again the results are consistent with the analytical picture presented here for $\tau > \tau_{min}$.

A third geometry of some interest is that of the biconic line shown in Figure 7(a). This example is also given in Reference 2. We take $Z_1 = 5.24\ \Omega$, $Z_2 = 15.7\ \Omega$, $\alpha = 95°$, $\beta = 90°$, $\gamma = 75.2°$, $x = 0$, $\ell = 200$ cm, $d = 20$ cm. Reference 5 treats only straight-sided radial lines, but since α and γ are not very different from 90°, we will use equivalent-circuit parameters from that source as a reasonable approximation. We find

$$C_1 = 107 \text{ pf}$$

$$C_2 = 37.7 \text{ pf}$$

$$C_3 = -26.4 \text{ pf}$$

$$L = 13.9 \text{ nh.}$$

---

[7] *R. Shnidman, "Computer Simulation of Electron-Beam-Cavity Interactions in Coaxial Geometry," BRL Report (to be published).*

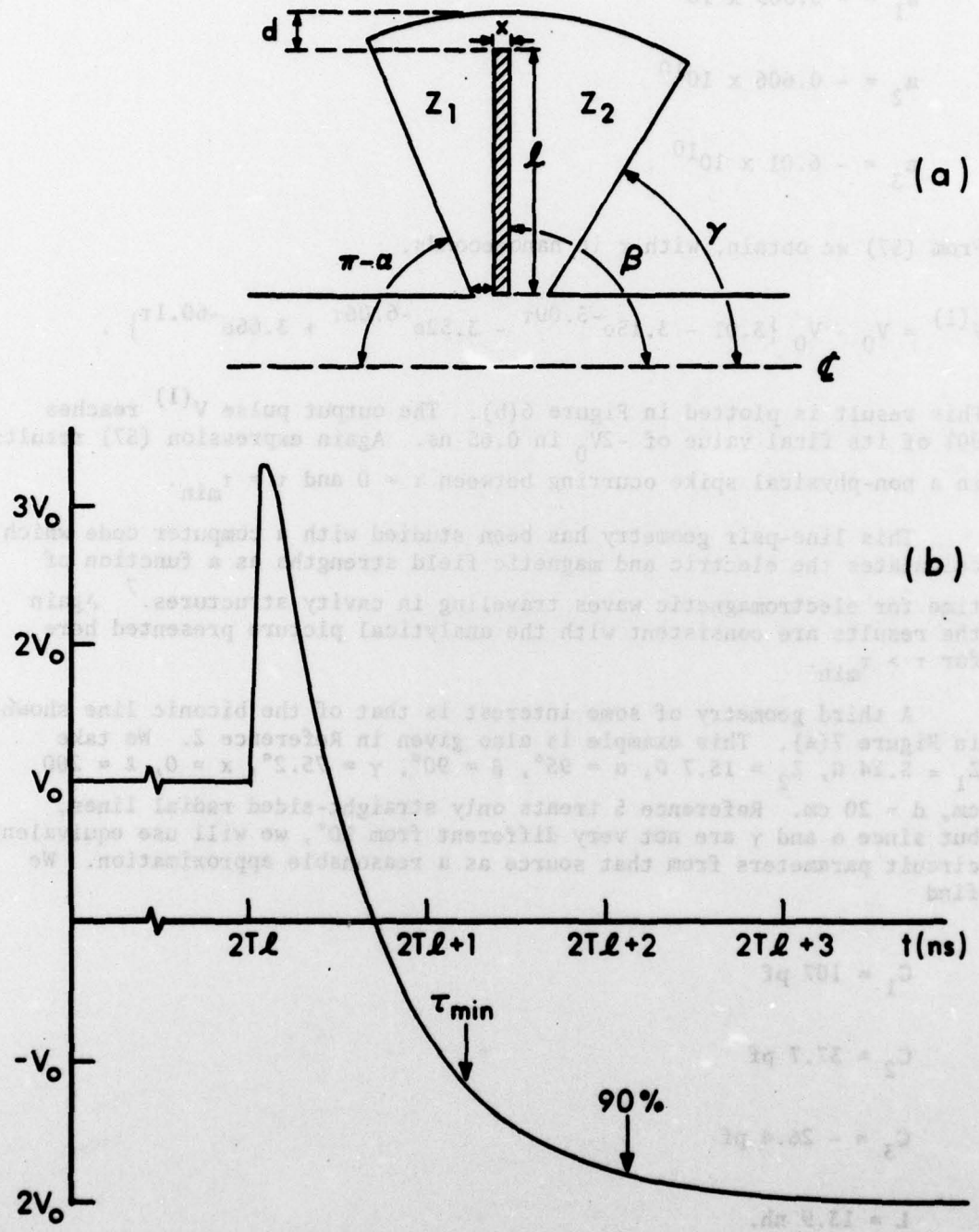

Figure 7. (a) Asymmetric biconic radial-line pair. (b) Open-circuit output pulse $V^{(1)}$.

Expression (38) for this case is

$$A(s) = s^3 + 3.44 \times 10^{10}\, s^2 + 1.07 \times 10^{20}\, s + 0.0864 \times 10^{30}$$

and the roots of $A(s) = 0$ are

$$a_1 = -1.50 \times 10^{10}$$

$$a_2 = -1.86 \times 10^{10}$$

$$a_3 = -3.10 \times 10^{10} .$$

From (57) we then obtain with τ in nanoseconds

$$V^{(1)} = V_0 - V_0 \{3 - 2.85e^{-1.50\tau} - 3.58e^{-1.86\tau} + 3.43e^{-31.0\tau}\} .$$

This result is plotted in Figure 7(b). The output pulse $V^{(1)}$ reaches 90% of its final value of $-2V_0$ at $\tau = 2.1$ *ns*. The positive spike is non-physical. Because of its rather intractable geometry, this case has not yet been studied either experimentally or through computer simulation of the electromagnetic fields.

A number of transmission-line equivalent-circuit cases, including the three examples given above, have been run on the network analysis computer code NET-2. While some difficulty has been encountered with numerical instabilities in the output, the results are in general agreement with those obtained from the foregoing Laplace-transform analysis.

4. SUMMARY

A Laplace-transform solution for an equivalent circuit representing the coupling region which occurs in internally-switched transmission-line-pair accelerator cavities has been derived. The results show that for a step-function input the effect of the coupling-region equivalent circuit on the open-circuit output voltage is a risetime deterioration which becomes increasingly severe with succeeding output pulses. Specific examples have been presented for three cavity geometries showing the risetime deterioration of the first output pulse.

ACKNOWLEDGEMENTS

The author is indebted to Dr. D. Eccleshall (BRL) for guidance and support in all phases of this work. Thanks are due to A. Kehs and R. Puttkamp of the Harry Diamond Laboratories for running the computer code NET-2.

REFERENCES

1. J.K. Temperley and D. Eccleshall, "Analysis of Transmission-Line Accelerator Concepts," Technical Report ARBRL-TR-02067, May 1978. (AD #A056364)
2. D. Eccleshall and J.K. Temperley, "Transfer of Energy From Charged Transmission Lines with Applications to Pulsed High-Current Accelerators," J. Appl. Phys., Vol. 49, No. 7, pp. 3649-3655, July 1978.
3. J.R. Whinnery and H.W. Jamieson, "Equivalent Circuits for Discontinuities in Transmission Lines," Proc. IRE 32, 98-115, 1944.
4. J.R. Whinnery, H.W. Jamieson, and T.E. Robbins, "Coaxial-Line Discontinuities," Proc. IRE 32, 695-709, 1944.
5. J.R. Whinnery and D.C. Stinson, "Radial Line Discontinuities," Proc. IRE 43, 46-51, 1955.
6. C.E. Hollandsworth, BRL Report (to be published).
7. R. Shnidman, "Computer Simulation of Electron-Beam-Cavity Interactions in Coaxial Geometry," BRL Report (to be published).

DISTRIBUTION LIST

No. of Copies	Organization
12	Commander Defense Documentation Center ATTN: DDC-TCA Cameron Station Alexandria, VA 22314
1	Commander US Army Materiel Development and Readiness Command ATTN: DRCDMD-ST, N. Klein 5001 Eisenhower Avenue Alexandria, VA 22333
1	Commander US Army Aviation Research and Development Command ATTN: DRSAV-E P. O. Box 209 St. Louis, MO 63166
1	Director US Army Mobility Research and Development Laboratory Ames Research Center Moffett Field, CA 94035
2	Commander US Army Electronics Research and Development Command Technical Support Activity ATTN: DELSD-L DRSEL-TL-BG, Dr. Schneider Fort Monmouth, NJ 07703
1	Commander US Army Communications Rsch and Development Command ATTN: DRDCO-PPA-SA Fort Monmouth, NJ 07703
1	Commander US Army Missile Research and Development Command ATTN: DRDMI-R Redstone Arsenal, AL 35809
1	Commander US Army Missile Materiel Readiness Command ATTN: DRSMI-AOM Redstone Arsenal, AL 35809
1	Commander US Army Tank Automotive Research & Development Cmd ATTN: DRDTA-UL Warren, MI 48090
3	Commander US Army Armament Research and Development Command ATTN: DRDAR-TSS (2 cys) DRDAR-TD, Dr. Weigle Dover, NJ 07801
1	Commander US Army Armament Materiel Readiness Command ATTN: DRSAR-LEP-L, Tech Lib Rock Island, IL 62199
4	Commander US Army Harry Diamond Labs ATTN: DELHD-RBC, Dr. Bromborsky Dr. A. Kehs Dr. R. Puttkamp DELHD-PP, Dr. Sokoloski 2800 Powder Mill Road Adelphi, MD 20783

DISTRIBUTION LIST

No. of Copies	Organization
1	Commander US Army Foreign Science and Technology Center ATTN: Dr. Thomas Caldwell 220 Seventh Street, NE Charlottesville, VA 22901
1	Director US Army TRADOC Systems Analysis Activity ATTN: ATAA-SL, Tech Lib White Sands Missile Range NM 88002
1	HQDA (DAMA-ARZ-A, MAJ Acklin) Washington, DC 20310
1	HQDA (DAMA-CSM-CS, LTC Townsend) Washington, DC 20310
1	Commander US Army Research Office ATTN: Dr. Herman Robl P. O. Box 12211 Research Triangle Park NC 27709
2	Director US Army BMD Advanced Technology Center ATTN: ATC-D, Dr. L.J. Havard Dr. T. Roberts P. O. Box 1500 Huntsville, AL 35807
1	US Army Research and Standardization Group (Europe) ATTN: Dr. Alfred K. Nedoluha Box 65 New York, FPO 09510
1	Commander Naval Surface Weapons Center ATTN: Code WR-401 Dr. C. M. Huddleston Silver Spring, MD 20910
2	Commander Naval Research Laboratory ATTN: Code 77002 Dr. M. Friedman Dr. J. Siambis Washington, DC 20375
1	AFWL (LTC Havey) Kirtland AFB, NM 87117
1	National Bureau of Standards ATTN: Dr. J. Leiss Director, Center for Radiation Research Room 229, Bldg. 245 Washington, DC 20234
1	Director ATTN: J. C. Nall P. O. Box 1925 Washington, DC 20505
2	Director Lawrence Livermore Laboratory ATTN: L-306, Dr. R. J. Briggs L-306, Dr. T. Fessenden University of California P. O. Box 808 Livermore, CA 94550
2	Director Sandia Laboratories ATTN: Dr. B. Miller, Fusion Rsch Department Dr. K. Prestwich, Pulsed Power Applications & Operations Division Albuquerque, NM 87115

DISTRIBUTION LIST

No. of Copies	Organization
1	Austin Research Associates, Inc. ATTN: Dr. L. Sloan 600 West 28th Street Austin, TX 78705
1	Battelle Columbus Laboratories ATTN: Dr. C. T. Walters Associate Manager, Physical Sciences Section 505 King Avenue Columbus, OH 43201
1	JAYCOR ATTN: Dr. M. Dowe 205 South Whiting Street Suite 500 Alexandria, VA 22304
1	Maxwell Laboratories, Inc. ATTN: Dr. Trivelpiece 9244 Balboa Avenue San Diego, CA 92123
2	Physical Dynamics, Inc. ATTN: Dr. K. Brueckner Mr. John Shea P. O. Box 556 La Jolla, CA 92038
1	Physics International Company ATTN: Dr. Sid Putnam 2700 Merced Street San Leandro, CA 94577
1	Rand Corporation ATTN: Dr. S. Kassel 2100 M. Street, NW Washington, DC 20002
1	R&D Associates ATTN: Dr. L. J. Delaney Asst Director of Corporate Development 1815 North Ft. Myer Drive Arlington, VA 22209
2	Science Applications, Inc. ATTN: Dr. M. P. Fricke Dr. R. Shanny 1200 Prospect Street La Jolla, CA 92037
1	Science Applications, Inc. ATTN: Dr. R. Johnston 2680 Hanover Street Palo Alto, CA 94304
1	Ian Smith, Inc. ATTN: Dr. I. Smith 3115 Gibbons Drive Alameda, CA 94501
1	University of California Lawrence Berkeley Laboratory ATTN: Dr. Dennis Keefe Berkeley, CA 94720
1	University of California School of Engineering and Applied Science ATTN: Prof. C. T. Leondes, Engineering Systems Dept Los Angeles, CA 90027
	Aberdeen Proving Ground
	Dir, USAMSAA Cdr, USATECOM ATTN: DRSTE-SG-H